Rare Earth Oxyfluorosulfides: A New Class of Compounds with Modulated Structure

Damien Pauwels,[†] François Weill,[†,‡] Alain Tressaud,[†] and Alain Demourgues*[,†]

ICMCB-CNRS, 87 avenue du Dr A. Schweitzer, 33608 Pessac Cedex, France, and CREMEM Université Bordeaux 1, 351 cours de la libération, 33405 Talence Cedex, France

Received May 20, 2005. Revised Manuscript Received October 13, 2006

New rare earth oxyfluorosulfides with $La_{4-x}Y_xO_2F_2S_3$ ($x = 0, 1, 2$) composition have been prepared by solid-state reactions. The structures of these compounds vary according to the x value. $La_4O_2F_2S_3$ exhibits an incommensurately modulated structure that has been investigated by means of powder X-ray and electron diffraction. The modulated structure has an orthorhombic symmetry, space group *Amam-(00γ)ss0* in (3 + 1) formalism with the following parameters $a = 7.0250(4)$ Å, $b = 7.2171(4)$ Å, $c = 4.2696(3)$ Å, and $q^* = 0.26070(5)$ c*. A three-dimensional approximation of the structure can be proposed by considering a superstructure of the basic cell with $c_1 = 23$ c. $La_{4-x}Y_xO_2F_2S_3$ ($x = 1, 2$) compounds exhibit commensurate networks related to a $Ce_4O_4S_3$ type structure and have been solved from X-ray powder diffraction data. These new phases exhibit ribbons and are closely related to the La_2O_2S type phases. The formation of these phases and the structural arrangements are explained by shearing mechanisms from the La_2O_2S structure. The origin of the modulation is discussed in terms of sheet arrangements and the local environment of the rare earth compound. Thus, it has been shown for the first time that the rare earth compound size, i.e., the nature, the number of neighbors, and the cation−anion bond distances, strongly influence the setting up of such modulations that occur to support constraints around the rare earth compound.

Introduction

Rare-earth-based oxysulfides and fluorosulfides have been largely studied and exhibit optical properties such as luminescence in $Y_2O_2S:Eu^{3+}$,[1] or $Gd_2O_2S:Tb^{3+}$,[2] or absorption in the visible range in $Ln_{10}S_{14}O$[3] or LnSF.[4] The nature of the rare earth compound as well as its local environment and the structural features of these compounds allow researchers to propose band schemes and electronic mechanisms at the origin of absorption properties.[4] Rare-earth-based, mixed-anion (O, S, F) compounds have recently been investigated in order to tune the environment of the rare earth, thus modifying optical absorption properties.[5,6] Indeed, the presence in the vicinity of rare earth ions (4f and 5d shells) of more than two anions (p shell) with various polarizabilities leads to an alteration of the energetic parameters such as the bandwidth and the position of the p and 5d bands, as well the position of 4f levels in the gap. Thus, the related absorption threshold can be shifted by playing with the nature and the number of anions around the rare earth.

Most of rare-earth-based, mixed-anion compounds exhibit layer structures due to the presence of anions with various polarizabilities. The sheet composition and their arrangments vary as a function of the nature and number of anions. The blocks containing oxygen and/or fluorine atoms depend on the relaxation and the number of succesive sulfur sheets. In rare-earth oxysulfides containing a single sulfur layer and deriving from Ln_2O_2S, cations and oxygens are almost distributed in the same planes with a close-packed stacking.[7] On the other hand, in oxysulfides and fluorosulfides that exhibit more than one successive sulfur sheet, cations and small anions (O, F) are localized on two different planes.[8] The increase in the number of sulfur sheets and the constraints inside leads to relaxing of the rare earth small anion (O,F) blocks.[6] Thus, a study has been devoted to the evolution of structural properties of the new rare earth oxyfluorosulfides series as a function of the Ln/S molar ratio, i.e., the number of succesive sulfur sheets. The system $La_2O_3-La_2S_3-LaF_3$ led us to synthesize $La_3OF_3S_2$ and $La_2O_{1.5}FS$, which present two different absorption onset (3.1 and 4.1 eV, respectively). $La_3OF_3S_2$ crystallized with the PbFCl type structure and can be described as a stacking of $[La_3OF_3]^{4+}$ fluorite type blocks and $[S_2]^{4-}$ double sulfur layers. The rare earth ion is located at the center of distorted square antiprisms with four F atoms in one base and four S atoms in the other. A fifth La−S bond appears in the apical position in relation to the lanthanum. The $La_2O_{1.5}FS$ compounds have a hexagonal structure deriving from La_2O_2S

* Corresponding author. Tel.: 33-5-40-00-26-55. Fax: +33-5-40-00-27-61. E-mai: demourg@icmcb.u-bordeaux.fr.
[†] ICMCB-CNRS.
[‡] CREMEM Université Bordeaux 1.

(1) Sovers, O. J.; Yoshioka, Y. *J. Chem. Phys.* **1968**, *49* (11), 4945−4954.
(2) Holsä, J.; Leskelä, M.; Niinistö, L. *Mater. Res. Bull* **1979**, *14*, 1403−1409.
(3) Besançon, P. *J. Solid State Chem.* **1973**, *7*, 232−240.
(4) Demourgues, A.; Tressaud, A.; Laronze, H.; Macaudiere, P. *J. Alloys Compd.* **2001**, *323−324*, 223−230.
(5) Pauwels, D.; Demourgues, A.; Tressaud, A. *Mater. Res. Soc. Symp. Proc.* **2003**, 755.
(6) Pauwels, D.; Demourgues, A.; Laronze, H.; Gravereau, P.; Guillen, F.; Isnard, O.; Tressaud, A. *Solid State Sci.* **2002**, *4*, 1471.
(7) Morosin, B.; Newman, D. J. *Acta Crystallogr., Sect. B* **1973**, *29*, 2647.
(8) Flahaut, J. *J. Solid State Chem.* **1974**, *9*, 124.

10.1021/cm0510817 CCC: $33.50
Published on Web 11/22/2006

with extra O/F anions. Its atomic arrangement involves $[La_2O_{1.5}F]^{2+}$ and a single sulfur layer. The lanthanum ion is surrounded by three sulfur atoms and four F/O atoms. It has been shown that the size as well as the charge of ionic blocks and finally the local environmment of the rare earth atom can vary.[6] Thus, the stabilization of ionic blocks with a 3+ charge has been attempted. In this case, the succession of single, double, and/or triple sulfur layers is expected, allowing various relaxation of blocks containing small anions (O,F). A simple composition of the 3+ block could correspond to $[La_2OF]^{3+}$ associated with the chemical formula $La_4O_2F_2S_3$. Furthermore, because the $Ce_2O_{2.5}S$ compound containing mixed valences (Ce^{3+},Ce^{4+}) has the same structural features as the oxyfluorosulfide $La_2O_{1.5}FS$, the crystal structure of the new $La_4O_2F_2S_3$ compound has been compared to that of the $Ce_4O_4S_3$ ("$Ce^{3+}{}_2Ce^{4+}{}_2O_2O_2S_3$") oxysulfide described in the literature.[9,10] The substitution for La^{3+} ions of smaller cations such as Y^{3+} that exhibit the same ionic size than Ce^{4+} and the evolution of structural properties have then been undertaken. The variation of the local environment of the rare earth compounds in this series has been studied. In this article, the synthesis and the characterization of new lanthanum-yttrium oxyfluorosulfides $La_{4-x}Y_xO_2F_2S_3$ ($x = 0$, 1, 2) have been reported.

Experimental Section

1. Preparation of Compounds and Chemical Analysis. $La_{4-x}Y_xO_2F_2S_3$ rare earth oxyfluorosulfides were synthesized by reaction of stoichiometric amounts of high-purity rare earth sulfides in their α form (Rhodia, 99.99%), rare earth fluorides, and rare earth oxides (Rhodia, 99.99%). To prepare fluorides, we have treated rare earth oxides with HF solution at 80 °C and then annealed them under anhydrous HF at 500 °C for 12 h. These starting materials were mixed under a dry argon atmosphere in a glove box because of their sensitivity to oxygen and moisture. The reactions were carried out in a platinum crucible placed in a quartz tube that was sealed under a vacuum and heated to 1200 °C for 48 h.

The amounts of fluorine and sulfur in the compounds have been determined by chemical analysis. In the case of fluorine, the samples have been dissolved in a flux of $CaCO_3/KCO_3$ at 800 °C and the amount of fluorine has been determined by using a LaF_3 specific electrode. For the sulfur determination, the samples were heated at 1300 °C, leading to the formation of SO_2. The quantity of SO_2 was measured by means of infrared spectroscopy, taking into account the pair of absorption bands represented by SO vibrations at 1360 ($\nu 3$) and 1151 cm^{-1} ($\nu 1$)[11] and their integrated areas compared with references. Thus, by chemical analysis, the following formulas $La_4O_{2.1}F_2S_{2.9}$ can be proposed, near the theoritical formula $La_4O_2F_2S_3$.

2. Electron and X-ray Diffraction Experiments. Transmission electron microscopy (TEM) experiments were performed with a JEOL 2000 FX microscope operating at 200 kV and using a side-entry, double-tilt specimen stage. The maximum tilt angles available are ±45°.

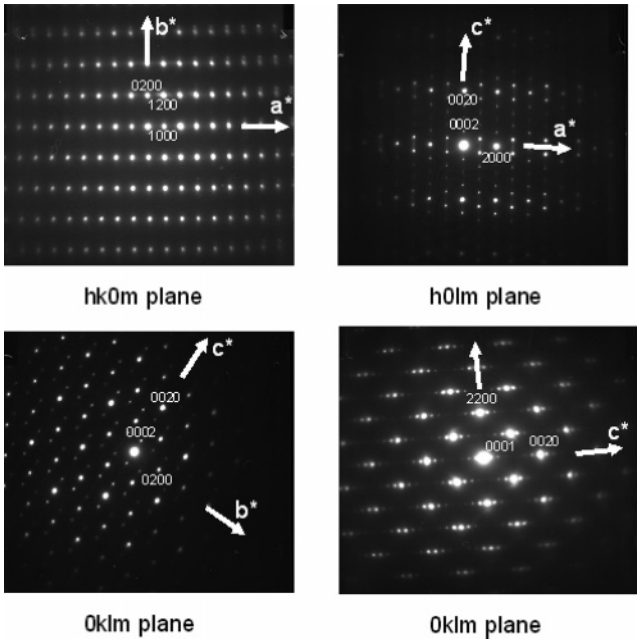

Figure 1. Electron diffraction patterns of $La_4O_2F_2S_3$ along various zone axis showing the incommensurate modulation.

Powder X-ray diffraction patterns of $La_{4-x}Y_xO_2F_2S_3$ ($x = 0$, 1, 2) phases were recorded on a Philips PW 1050 diffractometer in a Bragg−Brentano geometry, using monochromated Cu Kα radiation. Data were collected over $5° \leq 2\theta \leq 120°$ with 0.02° steps and an integration time of 30 or 40 s. The calculations for structural determinations were performed with a JANA2000[11] system or the Rietica package.[12] Reliability factors discussed in this paper were the usual ones defined by the Rietveld method.[13]

Results

1. Structural Determination of $La_4O_2F_2S_3$. A first analysis by X-ray and electron diffraction reveals the existence of an orthorhombic unit cell with average cell parameters $a \approx 7$ Å, $b \approx 7.2$ Å, $c \approx 17$ Å. On the basis of the XRD pattern, we find that the refined parameters correspond to $a \approx 7.02$ Å, $b \approx 7.23$ Å, $c \approx 17.07$ Å, but profile matching is not correct, especially at small angles. However, relationships with the unit cell of $Ce_4O_4S_3$ can be found: $a_{Ce} \approx a_{La,}$ $b_{Ce} \approx 2b_{La}$, $c_{Ce} \approx c_{La}/4$.

1.1. Electron Diffraction. The accurate observations of the electronic diffraction patterns along the [100] zone axis show the actual occurrence of strong and weak reflections, and the distances from each other are not equal along the c^* axis (Figure 1). It reveals that $La_4O_2F_2S_3$ has a modulated structure. The building of the reciprocal space from the electron diffraction patterns analysis leads to an orthorhombic cell with $a \approx 7$ Å, $b \approx 7.2$ Å, $c \approx 4.2$ Å and $q^* \approx 0.26$ c* described in (3 + 1) D formalism. The cell parameters have been refined on the basis of the X-ray powder diffraction pattern. The deduced values are $a = 7.0250(4)$ Å, $b = 7.2171(4)$ Å, $c = 4.2696(3)$ Å, and $q^* = 0.26070(5)$ c*. The experimental density $d_{exp} = 5.56$ is in good

(9) Dugué, J.; Carré, D.; Guittard, M. *Acta Crystallogr., Sect. B* **1978**, *34*, 3564.
(10) Dugué, J.; Carré, D.; Guittard, M. *Acta Crystallogr., Sect. B* **1979**, *35*, 1550.
(11) Petricek, V.; Dusek, M. *JANA2000 The Crystallographic Computing System*; Institute of Physics: Praha, Czech Republic, 2000.
(12) Hunter, B. A. *RIETICA Rietveld Analysis using a Visual Interface*; Australian Nuclear Science and Technologie Organisation: Menai, NSW Australia, 2001.
(13) McCusker, M. C.; Von Dreele, R. B.; Cox, D. E.; Louer, D.; Scardi, P. *J. Appl. Crystallogr.* **1999**, *32*, 36.

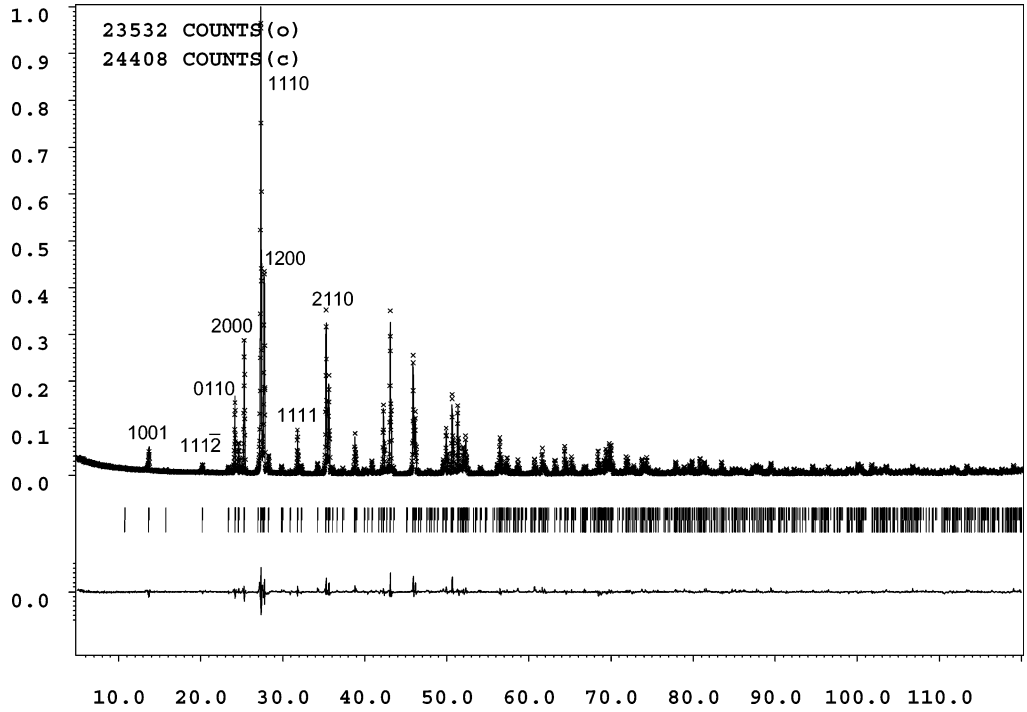

Figure 2. Observed (×) and calculated (full line) XRD patterns andthe difference curve of the $La_4O_2F_2S_3$ compound.

agreement with the calculated one ($d_{calcd} = 5.53$) for $Z = 1$ formula unit per unit cell. The study of various zone axes (Figure 1) allows us to determine the reflection conditions. These conditions are along the following planes: *0klm*, $k + l = 2n$ and $m = 2n$; *kklm*, $k + l = 2n$; *hk0m*, $k = 2n$; *h0lm*, $l = 2n$ and $h + m = 2n$, leading us to consider only two space groups, *Amam(00γ)ss0* (63.7) or *Ama2(00γ)ss0* (40.5).[14]

1.2. X-ray Powder Diffraction. The structure has been determined from the powder X-ray diffraction diagram recorded at room temperature (Figure 2). Diagrams corresponding to the $10° < 2\theta < 40°$ region for the modulated structure and without modulation are represented in Figure 3. Experimental data conditions are compiled in Table 1. First, the XRD profile of the $La_4O_2F_2S_3$ compound was refined, leading to the cell parameters reported in Table 2. XRD patterns have been also recorded at $T = 77$ and 10 K and the cell parameters change slightly, in good agreement with thermal expansion as confirmed in Table 2. No commensurate structures have been detected, even at low temperatures. The centrosymmetric *Amam(00γ)ss0* space group has been used to solve the structure. The main difficulty in this refinement has been in differentiating between oxygen and fluorine atoms. Thus, this analysis has been undertaken considering that these atoms were only oxygen atoms.

From the main reflections, atoms have been placed by considering conventional Patterson methods associated with a difference Fourier synthesis. Isotropic thermal displacement parameters were considered for all atoms.

The atomic position of the heavy element La was first determined and corresponds to a 4c($^1/_4$, *y*, 0) Wickoff position. Sulfur atoms occupy one 4a(0, 0, 0) site with an occupancy factor fixed to 0.75 according to the chemical composition. Oxygen/fluorine atoms are in the 8f(*x*, *y*, *z*) site, which is half occupied. These parameters describe the main reflections (R(all) = 12.67%, R_w(all) = 7.04%) quite well and have been used as a starting model for the refinement of the whole modulated structure. Because anionic sites are not fully occupied, a trial harmonic occupation function has been used to describe the occupancy of the sites. After some refinement cycles, it appears that a more efficient way was to use crenel functions centered at $t = 0$ for S and $t = 0.5$ for O/F. The reliability factors decrease, and the refined lengths of these functions are equal to 0.74(1) for sulfur atoms and 0.53(1) for oxygen/fluorine atoms, leading to a chemical formula, $La_4S_{2.96}(O,F)_{4.24}$, close to that determined by chemical analysis. Displacive modulation functions were then introduced for all atoms. The final parameters of these functions are reported in Table 3, with the whole atomic modulation functions being represented in Figure 4. At this last stage of the refinement, the reliability factors are $R_p = 9.33\%$, $R_{wp} = 12.79\%$, $R = 4.28/7.56\%$, and $R_w = 3.50/7.44\%$ for main peaks and first-order satellites, respectively. The global reliability factors are R(all) = 6.94% and $R_w = 6.04\%$. Final parameters are reported in Table 1. The final isotropic thermal displacements exhibit high error factors for S and O/F atoms. This is likely due to the complexity of the modulated structure refinement performed on the basis of powder diffraction data.[15] These experimental data are indeed less accurate than the single-crystal diffraction data. Moreover, the simultaneous effects of displacive and occupation modulation functions on O/F and S atoms contribute to the increase in these incertitudes.

To confirm the refinement, we undertook the analysis of the interatomic distances as a function of the *t* coordinate along the direction perpendicular to the 3D space (Figure

(14) *International Tables for Crystallography*; International Union of Crystallography: Chester, U.K., 1992; Vol. C, p 797.

(15) Dusek, M.; Petricek, V.; Wunchel, M.; Dinnebier, R. E.; van Smaalen, S. *J. Appl. Crystallogr.* **2001**, *34*, 398.

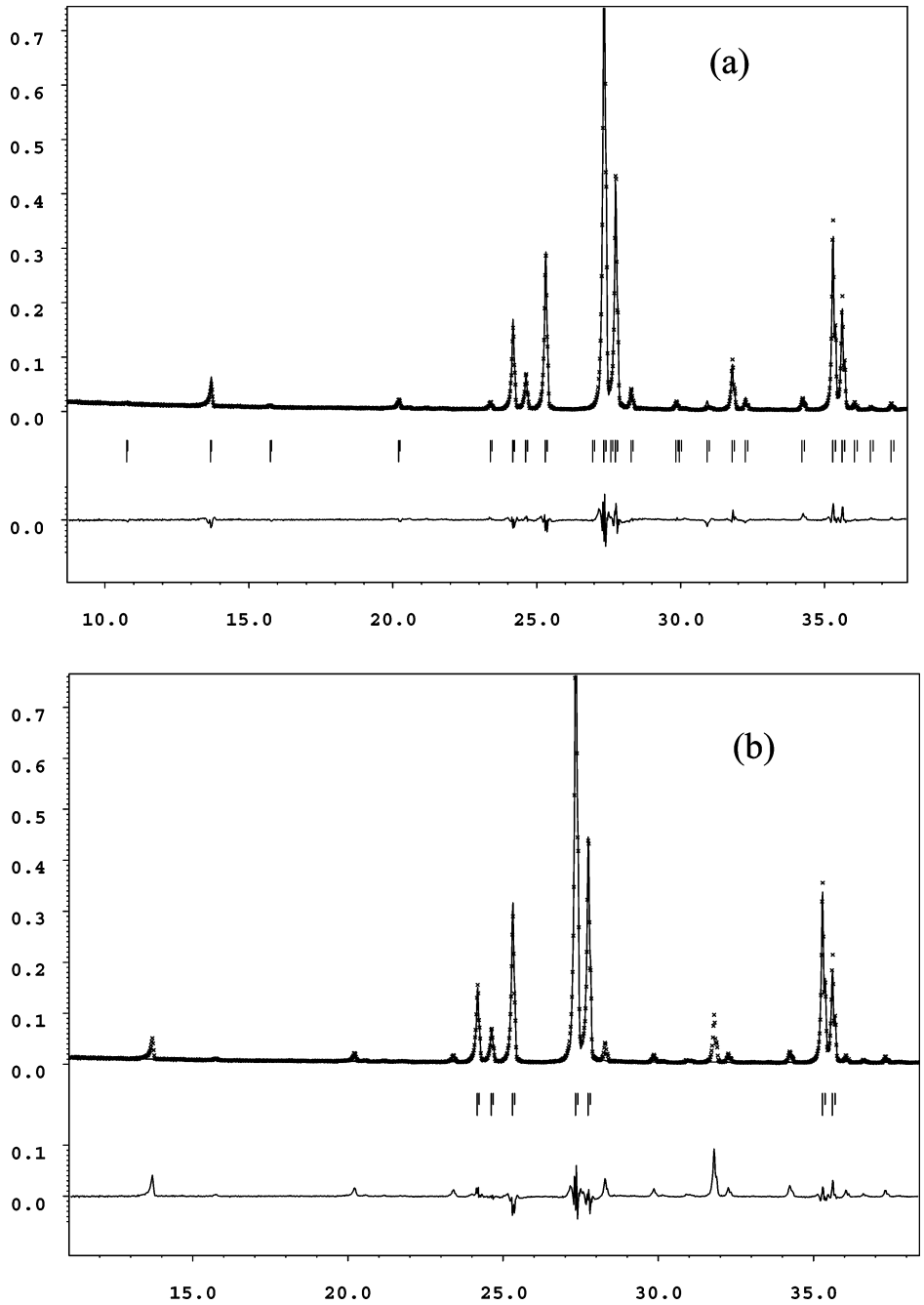

Figure 3. Observed (×) and calculated (full line) XRD patterns and the difference curve of the $La_4O_2F_2S_3$ compound corresponding to the $10° < 2\theta < 40°$ region, considering the modulated structure and without the modulation.

5). The average distances ($d_{La-S} \approx 3.05$ Å, $d_{La-O/F} \approx 2.45$ Å, $d_{O/F-S} \approx 3.25$ Å, $d_{O/F-O/F} \approx 2.85$ Å) are comparable to that observed in rare earth oxysulfides (Ln_2O_2S type)[7] and fluorosulfides (α-LnSF type).[4,16] However, the smallest bond distances, d_{min}, for La−S (2.75 Å) and La−O/F (2.30 Å) are short. Nevertheless, these values are reported in $Ce_4O_4S_3$[9] and $Ce_6O_6S_4$[10] cerium oxysulfides. The smallest bond lengths $d_{min,O/F-O/F}$ (2.35 Å) and $d_{min,S-O/F}$ (2.85 Å) seem very short if the ionic radius of these atoms ($r(O^{2-}) = 1.4$ Å; $r(F^-) = 1.33$ Å; $r(S^{2-}) = 1.84$ Å, with coordinence equal to 6) are taken into account. However, such short bond distances have already been observed in the $LaF_{1.70}O_{0.65}$ compound, whose structure has been solved from powder neutron diffraction data[17] ($d_{O-F} = 2.34-2.43$ Å). Finally, in lanthanum−titanium oxysulfides and oxychlorosulfides,[18,19] the S−O bond lengths are equal to 2.9 Å. Thus, the interatomic distances determined from the structure refinement of the $La_4O_2F_2S_3$ compound have been largely observed in the literature.

The local environment of lanthanum atoms can be determined on the basis of the evolution of the La−S and La−O/F distances versus *t* (Figure 6). Different areas are defined in Figure 5. They correspond to the domains of existence of the six possible lanthanum environments. From

(16) Schleid, T.; Grossholz, H. *Anorg. Z. Allg. Chem.* **2001**, *627*, 2693.

(17) Laval, J. P.; Abaouz, A.; Frit, B.; Roult, G.; Harrison, W. T. A. *Eur. J. Solid State Inorg. Chem.* **1998**, *t25*, 425.

(18) Cody, J. A.; Ibers, J. A. *J. Solid State Chem.* **1995**, *114*, 406.

(19) Palvadeau, P.; Boyer, M. C.; Meerschaut, A.; Rouxel, J. *J. Solid State Chem. 139* **1998**, 220.

Table 1. Experimental Conditions and Refined Parameters of Powder X-ray Diffractograms of $La_{4-x}Y_xO_2F_2S_3$ ($x = 0, 1, 2$) Compounds

	$La_4O_2F_2S_3$	$La_3YO_2F_2S_3$	$La_2Y_2O_2F_2S_3$
diffractometer		Philips PW 1050, Bragg-Bentano geometry	
radiation		$\lambda_1 = 1.54051$ Å; $\lambda_2 = 1.5433$ Å	
2θ angular range (deg)	5−120	5−100	5−100
step (deg), time per step (s)	0.02, 40	0.02, 30	0.02, 30
refinement program	JANA2000	Rietica 1.77	Rietica 1.77
no. of background params	10 (Legendre function)	6 (Cheybshev function)	6 (Cheybshev function)
sample displacement	3.17(28)	−0.170(1)	−0.091(2)
symmetry		orthorhombic	
space group	*Amam*(00γ)*ss*0	*Pbam*	*Pbam*
a (Å)	7.0250(4)	6.9444(1)	6.8106(1)
b (Å)	7.2171(4)	14.9425 (2)	14.8932(4)
c (Å)	4.2696(3)	4.0614(1)	3.9571(3)
*q**	0.26070(5) c*		
V (Å^3), *Z*, D_{exp} (g cm^{-3})	216.46(3), 1, 5.53(2)	421.44(1); 2	401.38(2); 2
mo. of refined params	42	33	30
profiles function: pseudo-Voigt	Thomson, Cox Hastings:	$U = 0.026(3)$,	$U = 0.0362(4)$,
	$U = 41(5)$,	$V = -0.004(2)$,	$V = -0.004(4)$,
	$V = -35(5)$,	$W = 0.0032(9)$,	$W = 0.0039(8)$,
	$W = 11(1)$,	$\eta = 0.73(2)$	$\eta = 0.79(2)$
	$X = 5.3(3)$,		
	$Y = -2.9(9)$		
reliability factors R_p/R_{wp} (%)	9.33/12.79; R(all) = 6.94 (4.28 main; 7.56 satellites), R_w(all) = 6.04 (3.59 main; 7.44 satellites)	12/15.3; R-Bragg = 8.02	11.2/14.9; R-Bragg = 6.60

Table 2. Refined (XRD Data) Cell Parameters of the $La_4O_2F_2S_3$ Compound at $T = 298$, 77, and 10 K

T (K)	*a* (Å)	*b* (Å)	*c* (Å)	|*q**|
293	7.0250(4)	7.2171(4)	4.2696(3)	0.26070(5)
77	7.0145(10)	7.2109(10)	4.2620(6)	0.26111(6)
10	7.0119(4)	7.2085(4)	4.2601(2)	0.26101(2)

the length of the areas, we can deduce the probability of occurrence of a given environment. Two of them are majority. The first one consists in a lanthanum atom surrounded by 4 O/F atoms and 4 sulfur atoms (occurrence: 40.4%), whereas in the second one (occurrence: 39%), an additional sulfur atom is present and the fourth oxygen appears at larger distances than or in the same range as the three other oxygens. In the former environment, the La−O/F bond lengths are in the 2.3−2.5 Å range, three La−S bonds vary between 2.9 and 3.2 Å, and the fourth bond is around 3.4 Å. In the latter environment, the variation in the La−S bond lengths is even larger (between 2.72 and 3.38 Å). Concerning the La−O/F distances, three of them are in the 2.29−2.82 Å range, whereas the fourth distance varies between 2.45 and 3.45 Å. It is worthwhile to note that in a very narrow area ($\Delta t = 0.003$) around $t = 0$ and $t = 0.5$, the La polyhedron (4 O/F atoms and 5 S atoms) is very regular, with a low dispersion of La−O/F and La−S bond distances (Figure 7). The third possible environment for the lanthanum atoms has an occurrence of 10.4%. It consists of 4 sulfur atoms with La−S bond distances between 2.85 and 3.35 Å and 5 O/F atoms, four of them at distances between 2.3 and 2.53 Å and the last one at a distance much more larger (3.49 Å $\leq d_{La-O/F} \leq$ 3.53 Å). The three other possible environments are minority. They consist of 5 S atoms and 5 O/F atoms (occurrence: 3.2%), 5 S atoms and 6 O/F atoms (occurrence: 3.2%), and 4 S atoms and 6 O/F atoms (occurrence: 3.8%).

2. Structural Determinations of $La_3YO_2F_2S_3$ and $La_2Y_2O_2F_2S_3$. The $La_{4-x}Y_xO_2F_2S_3$ ($x = 1$, 2) phases adopt an orthorhombic symmetry with the space group *Pbam* (No. 55) related to the $Ce_4O_4S_3$[9] structure. The powder X-ray diffractograms of these phases have been refined by the Rietveld method in order to acurately determine the atomic positions and isotopic thermal displacement. The results are given in Table 4. The agreement factors are rather small ($R = 6.60\%$ for $La_2Y_2O_2F_2S_3$ and $R = 8.02\%$ for $La_3YO_2F_2S_3$), despite the presence of a small amount of Y_2O_2S in the preparation of $La_3YO_2F_2S_3$ composition. La and Y are distributed in two sites. The 4h (*x*, *y*, 1/2) site is mainly occupied by the lanthanum. The 4g (*x*, *y*, 0) position is almost fully occupied (95%) by yttrium atoms in $La_2Y_2O_2F_2S_3$ and corresponds to the position of Ce(IV) in $Ce_4O_4S_3$.[9] This position is half occupied by yttrium and lanthanum in $La_3YO_2F_2S_3$. Sulfur atoms occupy two positions, 4g (*x*, *y*, 0) and 2e (0, 1/2, 1/2). O/F atoms are located in 4g (*x*, *y*, 0) and 4h (*x*, *y*, 1/2) positions. The isotropic thermal displacements of anions are fixed to 0.4 for sulfur atoms and 1 for oxygen/fluorine anions. Actually, only the isotropic displacements of cations with a quite high electronic density have been refined. The structure as well as the local environments of the rare earth ions are represented on Figure 8. The isotropic thermal displacements of the rare earth ions as well as the occupancies have been refined, taking into account some relationships, because of the strong correlation between both these parameters. Actually, the thermal displacements of 4h sites for La1 and Y1 are identical as well as for La2 and Y2 (4g sites), and the sum of occupancies in each site is constant and corresponds to fully filled sites. The main bond distances are reported in Table 5. The smaller bond distances (La−S = 2.93 Å, Y−S = 2.77 Å, La−O/F = 2.30 Å, Y−O/F = 2.20 Å, S−O/F = 3.18 Å, O(F)−O(F) = 2.76 Å) are quite comparable to thpse found in rare earth oxysulfides, oxyfluorides, and oxides. In the smaller rare earth site (Figure 7), Y and La are located in a 3-fold axis with a triangle of three sulfur atoms on one side (Y(La)−S bond distances vary between 2.77 and 3.03 Å) and a triangle of three O/F atoms (Y(La)−O/F bond distances vary between

Table 3. Atomic Positions, Isotropic Thermal Displacement, Occupancies, and Parameters of Displacive Modulation Functions for the $La_4O_2F_2S_3$ Compound

atom	site	*x*	*y*	*z*	*B* (Å^2)	*n*
La	4c	1/4	0.3316(3)	0	0.64(9)	1
S	4a	0	0	0	0.02(35)	0.74(1)
O/F	8f	0.1334(28)	0.6435(37)	0	0.7(7)	0.53(1)

Displacive modulation function

La atom (classical function): $r^{La}(x_4) = r_0^{La} + \sum_n [u_{s,n}^{La} \sin(2\pi n x_4) + u_{c,n}^{La} \cos(2\pi n x_4)]$

with $u_{s,n}^{La} = (A_{xs,n}^{La}, A_{ys,n}^{La}, A_{zs,n}^{La})$ and $u_{c,n}^{La} = (A_{xc,n}^{La}, A_{yc,n}^{La}, A_{zc,n}^{La})$

$A_{xsin,1}^{La}$	$A_{ysin,1}^{La}$	$A_{zsin,1}^{La}$	$A_{xcos,1}^{La}$	$A_{ycos,1}^{La}$	$A_{zcos,1}^{La}$
0	0	0	0.0372(4)	0	0
$A_{xsin,2}^{La}$	$A_{ysin,2}^{La}$	$A_{zsin,2}^{La}$	$A_{xcos,2}^{La}$	$A_{ycos,2}^{La}$	$A_{zcos,2}^{La}$
0	0	−0.036(1)	0	0.0211(5)	0

S and O/F atoms (orthogonalized function):

$r^{\nu}(x_4) = \sum_n u_n^{\nu} ortho_n^{\nu}(x_4)$ with $ortho_i^{\nu}(x_4) = B_0^{\nu} + \sum_n [A_n^{\nu} \sin(2\pi n x_4) + B_n^{\nu} \cos(2\pi n x_4)]$

S atom[a]	B_0^S	A_1^S	B_1^S	A_2^S	B_2^S
$ortho_0^S$	1				
$ortho_1^S$	0	1.284			
$ortho_2^S$	−0.552	0	1.821		
$ortho_3^S$	0	−0.244	0	1.442	
$ortho_4^S$	1.016	0	−1.863	0	2.118

O/F atom[b]	$B_0^{O/F}$	$A_1^{O/F}$	$B_1^{O/F}$
$ortho_0^{O/F}$	1		
$ortho_1^{O/F}$	0	1.414	
$ortho_2^{O/F}$	2.069	0	3.249

[a] For the S atom, $A_{zortho,1}^S = -0{,}077(2)$; $A_{zortho,3}^S = 0{,}041(4)$. [b] For the O/F atom, $A_{zortho,1}^{O/F} = 0.095(6)$; $A_{xortho,2}^{O/F} = -0.002(4)$; $A_{yortho,3}^{O/F} = -0.024(5)$.

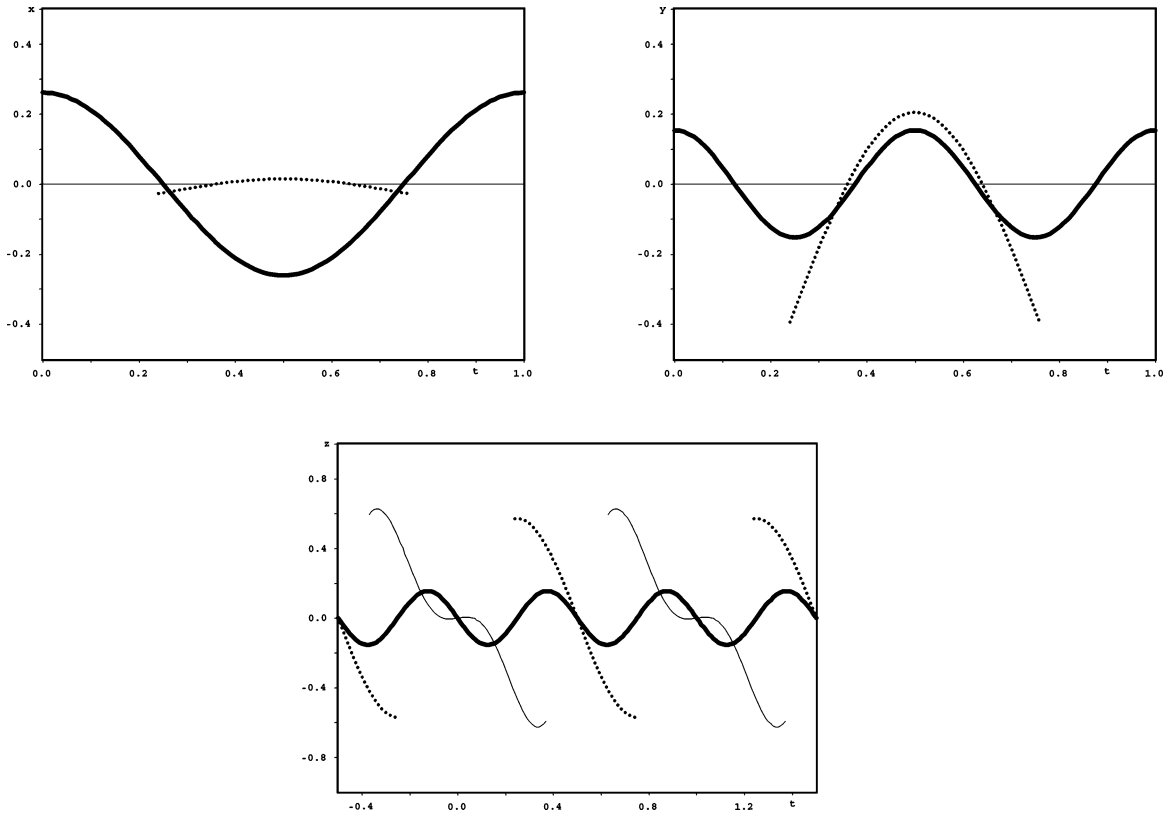

Figure 4. Atomic modulation functions for all atoms in $La_4O_2F_2S_3$ compound (lanthanum, bold lines; sulfur, normal lines; oxygen (fluorine), dotted lines). Variation of *x*, *y*, *z* coordinates as a function of the *t* parameter.

2.20 and 2.50 Å) and one axial O/F on the other side (Y(La)−O/F bond distances vary between 2.20 and 2.46 Å). A fourth S atoms appears at a larger bond length than the others ones (La−S ≈ 3.5 Å) and can be considered to be outside of the coordination polyhedra. The number of neighbors around the rare earth ion in this smaller site can be written 4O/F + (3 + 1)S. The other site that is larger (Figure 7) than the previous one and mainly occupied by La

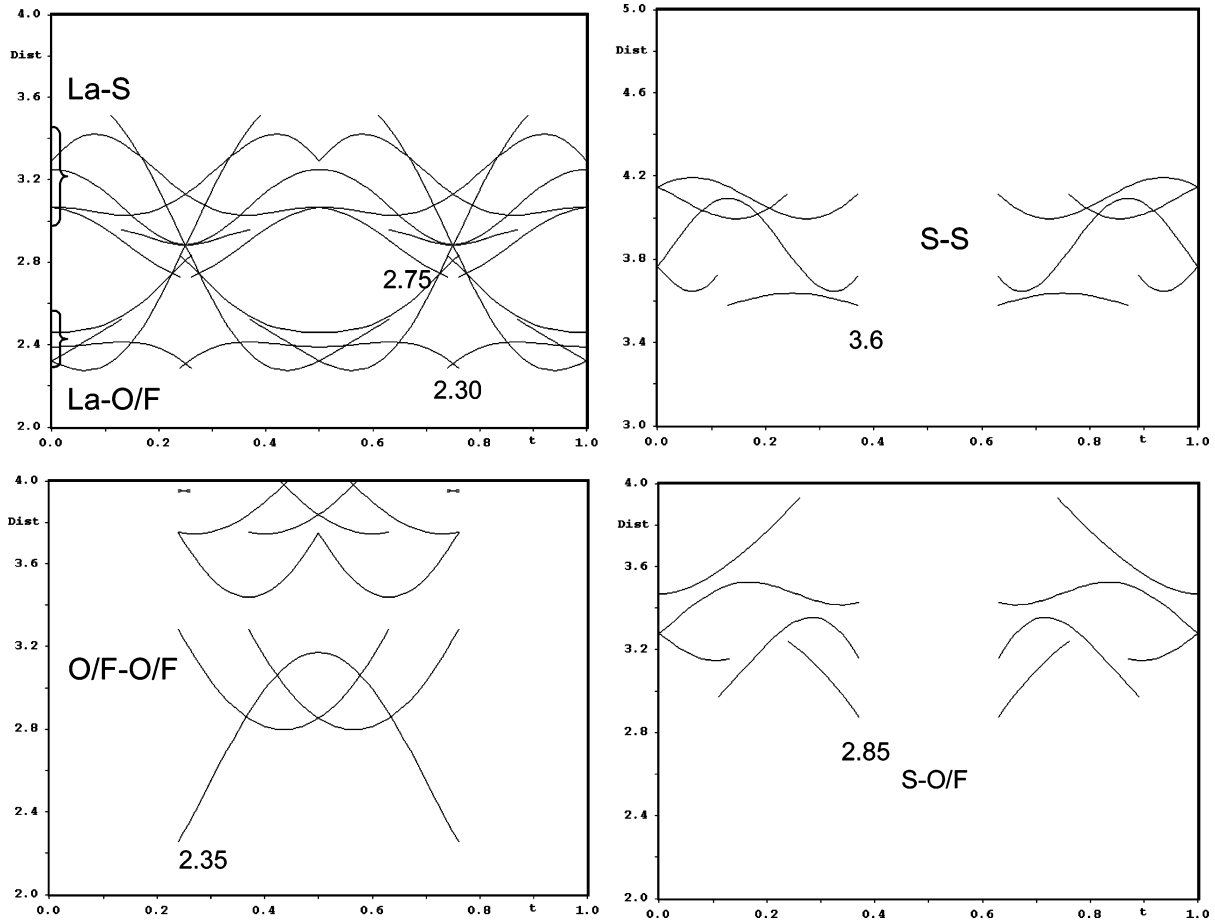

Figure 5. Variations of the main interatomic bond distances (La−X, O/F−O/F, S−S, S−O/F) vs *t* in the $La_4O_2F_2S_3$ compound.

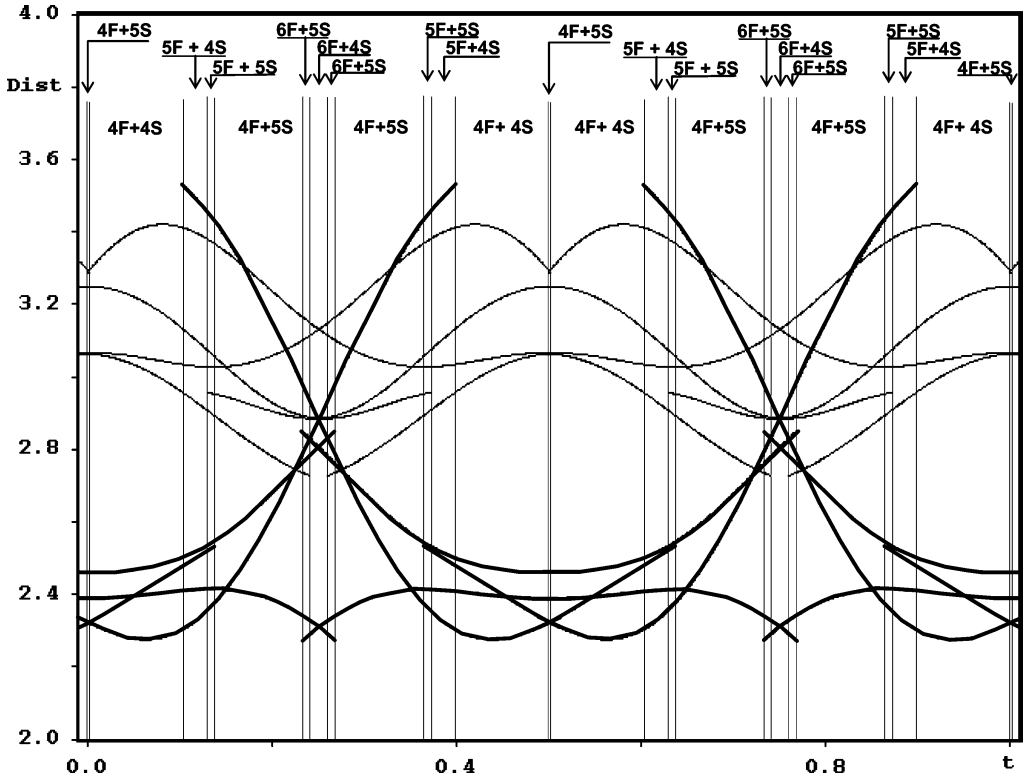

Figure 6. Variations of the La−X (X = S normal lines, O/F bold lines) bond distances vs *t* showing the areas corresponding to the feasible La environments with the evolution of the nature and number of neighbors along the modulation (*t*).

atoms is surrounded by five sulfur atoms (La−S bond distances vary between 2.96 and 3.14 Å) and three oxygen/fluorine atoms (Y(La)−O/F bond distances vary approximately between 2.33 and 2.55 Å). A fourth oxygen/fluorine

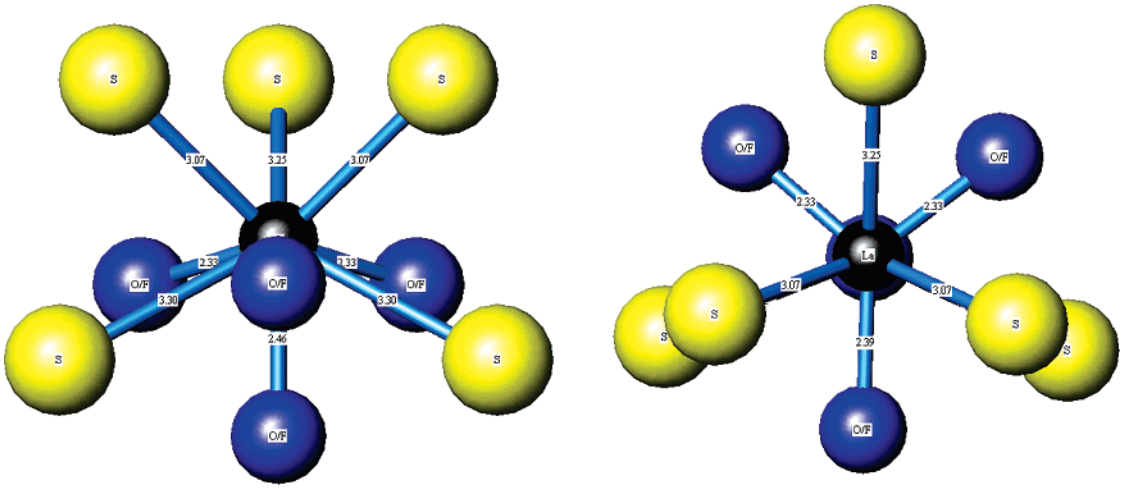

Figure 7. Representations of the La environment for $t = 0$ and $t = 0.5$.

Table 4. Atomic Positions, Isotropic Thermal Displacement, and Occupancies of $La_3YO_2F_2S_3$ and $La_2Y_2O_2F_2S_3$ Compounds

atom	site	*x*	*y*	*z*	*B* (Å^2)	*n*
		Atomic Positions $La_3YO_2F_2S_3$				
La1	4h	0.2219(3)	0.1660(1)	0,5	1.00(7)	0.92(2)
Y1	4h	0.2219(3)	0.1660(1)	0,5	1.00(7)	0.08(2)
La2	4g	0.2767(3)	0.4225(2)	0	0.92(8)	0.58(1)
Y2	4g	0.2767(3)	0.4225(2)	0	0.92(8)	0.42(1)
S1	4g	0.0096(9)	0.2805(4)	0	0.4	1
S2	2d	0	0.5	0.5	0.4	1
O/F1	4g	0.131(1)	0.074(1)	0	1	1
O/F2	4h	0.401(2)	0.3807(9)	0.5	1	1
		Atomic Positions $La_2YO_2F_2S_3$				
La1	4h	0.2278(2)	0.1633(1)	0,5	0.34(5)	0.95(2)
Y1	4h	0.2278(2)	0.1633(1)	0,5	0.34(5)	0.05(2)
La2	4g	0.2803(3)	0.4295(1)	0	0.36(8)	0.05(1)
Y2	4g	0.2803(3)	0.4295(1)	0	0.36(8)	0.95(1)
S1	4g	0.0299(1)	0.2828(3)	0	0.4	1
S2	2d	0	0.5	0.5	0.4	1
O/F1	4g	0.113(2)	0.0692(7)	0	1	1
O/F2	4h	0.366(1)	0.3671(9)	0.5	1	1

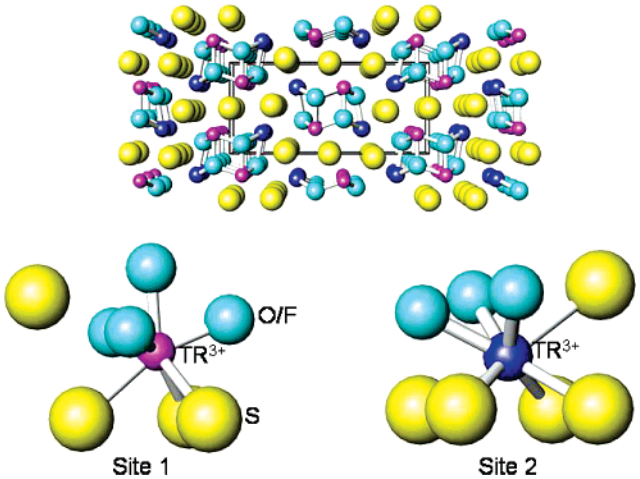

Figure 8. Structure and local environments of rare earth elements in $La_{4-x}Y_xO_2F_2S_3$ compounds.

atoms appears at larger distances at 3.18 Å ($La_2Y_2O_2F_2S_3$) and 3.44 Å ($La_3YO_2F_2S_3$). The number of neighbors around the rare earth ion in this larger site can be written as (3 + 1)O/F + (5)S.

Discussion

1. Three-Dimensional Approximation of $La_4O_2F_2S_3$ Structure. Origin of the Modulation. Because the modulus of the q^* vector along the c^* axis, equal to 0.2607, corresponds approximately to 6/23, a three-dimensional approximation of the structure can be proposed by considering a superstructure of the basic cell with $c_1 = 23$ c. The space group $A112/m$ corresponding to a monoclinic cell ($a_1 = 7.025$ Å, $b_1 = 7.217$ Å, $c_1 = 98.196$ Å, $\beta = 90.00$ °) and an origin shift equal to 2/23 can be used and leads to a representation close to the incommensurate modulated structure (Figure 8). Forty-three fully occupied atomic positions have to be taken into account in this supercell. As shown in Figure 9, the $La_4O_2F_2S_3$ network is constituted by ribbons with a complex geometry. Indeed, these ribbons can be describe as a repetition of $La_n(O/F)_n$ units corresponding to a stacking of La and small anions blocks perpendicularly to the *a* axis. Moreover, these units are separated by a single sulfur layer growing perpendicularly to the *a* axis. In the supercell, sulfur layers have a thickness corresponding to six or five S atoms along the *c* axis. The sequence in this average structure along the *c* axis can be described as the intergrowth of five blocks with six sulfur atoms and one block with five sulfur atoms. The evolution of the number of sulfur atoms along the *c* axis from 6 to 5 is associated with the variation in the ribbon size from the $[La_4(O/F)_4]_n$ unit to the $[La_3(O/F)_3]_n$ unit, respectively. Thus, the modulated structure of the $La_4O_2F_2S_3$ compound is due to the presence of shorter La ribbons associated with the reduction of sulfur atoms into S layers along the *c*-axis. The origin of these small blocks will be discussed later.

Thus, the description in the 4D space leads to two main local environments for the rare earth ions. In the first main

Table 5. Rare Earth Polyhedra (Main Interatomic Distances) in $La_3YO_2F_2S_3$ and $La_2Y_2O_2F_2S_3$ Compounds

Rare Earth Polyhedra (interatomic distances) in $La_3YO_2F_2S_3$			
La1/Y1−S1	3.037(6) × 2	La2/Y2−S1	2.818(6) × 1
La1/Y1−S1	2.958(6) × 2	La2/Y2−S2	3.026(5) × 2
La1/Y1−S2	3.1439(1) × 1	La2/Y2−O/F1	2.35(1) × 1
La1/Y1−O/F1	2.522(9) × 2	La2/Y2−O/F1	2.46(1) × 1
La1/Y1−O/F2	2.33(1) × 1	La2/Y2−O/F2	2.294(6) × 2
Rare Earth Polyhedra (interatomic distances) in $La_2Y_2O_2F_2S_3$			
La1/Y1−S1	2.983(4) × 2	La2/Y2−S1	2.772(6) × 1
La1/Y1−S1	2.964(4) × 2	La2/Y2−S2	2.942(1) × 2
La1/Y1−S2	3.058(1) × 1	La2/Y2−O/F1	2.20(1) × 1
La1/Y1−O/F1	2.545(6) × 1	La2/Y2−O/F1	2.27(1) × 1
La1/Y1−O/F2	2.502(5) × 2	La2/Y2−O/F2	2.263(5) × 2

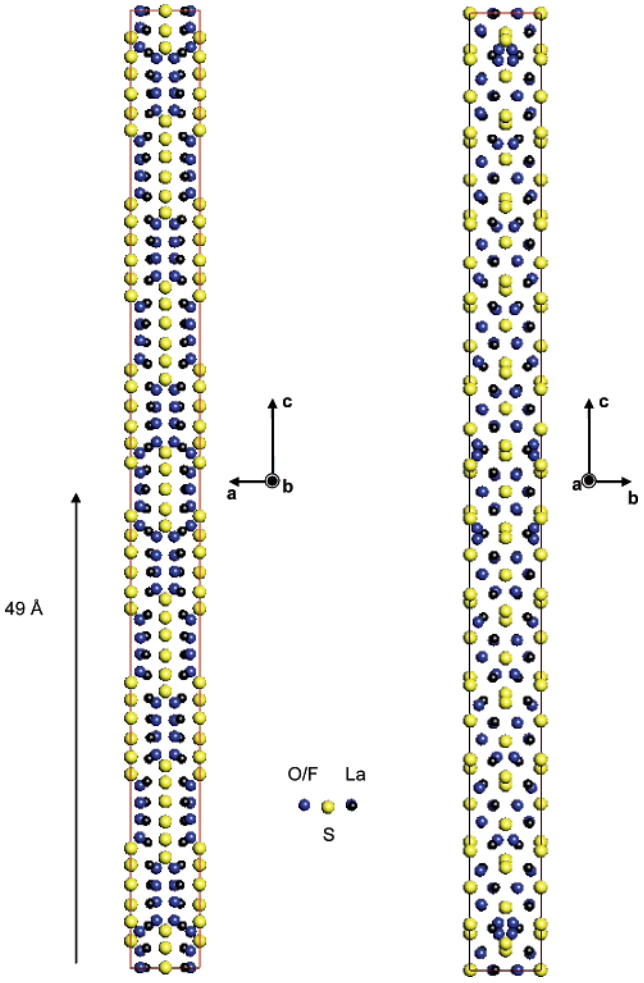

Figure 9. Representation of the 3D supercell of $La_4O_2F_2S_3$.

site (occurrence: 40.4%), lanthanum atoms are surrounded by four oxygen/fluorine atoms and four sulfur atoms. If this fourth, longer Ln−S bond length is not taken into account, the geometry of the coordination polyhedra is similar to that found in Ln_2O_2S[7] compounds. The second main kind (occurrence 39%) of the rare earth environment comprised five sulfur atoms, three O/F atoms, and a fourth O/F atoms at longer distances. The coordination polyhedra then correspond in this case to distorted square antiprisms. It is relevant to notice that these two anionic environments of the rare earth ions are almost similar to that observed in $Ce_4O_4S_3$ and $La_{4-x}Y_xO_2F_2S_3$ ($x = 1, 2$) (Figures 7 and 8). O/F atoms are surrounded by either a tetrahedra of four La atoms or three lanthanum atoms in a plane. Sulfur atoms are 6-fold coordinated and are located in a center of La octahedra with four La−S short distances around 3 Å and two longer ones around 3.3 Å. The modulation described along the *c* axis creates other environments close to both the previous environments. It is then interesting to focus on the evolution of La coordination polyhedra along the *c* axis and more precisely, the variation of the La−S and La−O/F bond distances versus the *t* coordinate in the 4D space or along a sequence of 23 polyhedra in the supercell, where this description is an approximate picture in 3D space of the incommensurate modulated structure. To clarify the discussion, we have followed the evolution of two main kinds of La polyhedra in this sequence. First, the smaller lanthanum

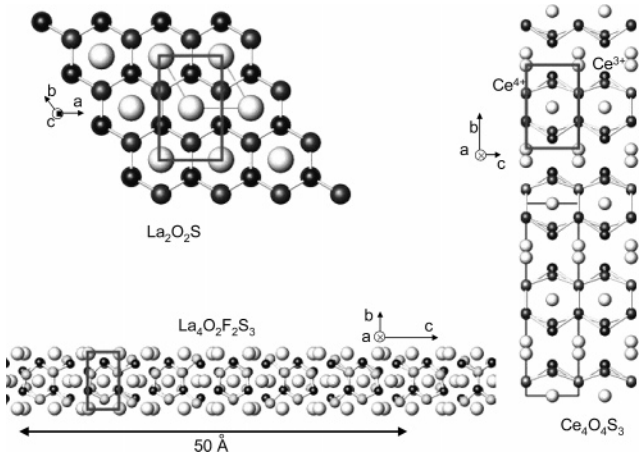

Figure 10. Representation of La_2O_2S, $Ce_4O_4S_3$, and $La_4O_2F_2S_3$ structures.

polyhedra constituted of 4 O/F atoms and 4 sulfur atoms remain almost identical. This site is close to that found in La_2O_2S.[7] However, the dispersion of La−S bond distances remains higher (2.95−3.45 Å) than that of La−O(F) distances (2.28−2.52 A). As far as the largest ones, constituted by (3 + 1) O/F atoms and 5 sulfur atoms, are concerned, these cationic sites exhibit outstanding differences. The longest La−O/F bond distance varies in the largest scale (2.45−3.45 A), whereas the longest La−S bond lengths exhibit smaller variations. For the other three La−O/F and four La−S distances, the dispersion increases and decreases periodically along this series. On the other hand, the La−O/F and La−S bond distances vary in the opposite. Finally, only two large sites along this sequence of polyhedra ($t = 0$ and $t = 0.5$) exhibit a low dispersion of the four La−O/F bond distances (2.33−2.45 Å) and the five La−S distances (3.08−3.30 Å). These two sites correspond to the minima of the La−X bond length dispersion, starting points where the modulation can grow. Thus, only the largest sites seem to be strongly affected by this modulation. The evolution of the bond lengths in this polyhedra series will be discussed in connection with the other related compounds that adopt a commensurate structure.

2. Structural Relationships between $La_{4-x}Y_xO_2F_2S_3$ (x = 0, 1, 2) and La_2O_2S. Structural studies reveal a strong correlation between $La_4O_2F_2S_3$, $Ce_4O_4S_3$, and La_2O_2S networks. In these networks, hexagonal cells constituted by Ln and O/F atoms with S atoms located in the center can be identified. A tetragonal network with S atoms at the corners, represented in Figure 10 with a thick rectangle, appears in these structures. The structural relationship between Ln_2O_2S and $Ce_4O_4S_3$ has been previously described by Dugué et al.[9] The authors suggest a shear mechanism in order to explain the formation of $Ce_4O_4S_3$ from Ce_2O_2S structures.

The different networks can be represented on the basis of the stacking of previous tetragonal cells (Figure 11). In $Ce_4O_4S_3$, a shear operation occurs along the $(010)_h$ plane (dot line (**1**)) of each hexagonal unit cell of Ce_2O_2S, with a $^1/_2\ c_h$ vector translation. This shear mechanism can be also described on the basis of the previous tetragonal unit cell and operate in this reference along the $(010)_t$ plane with a $^1/_2\ a_t$ vector translation. Each shear mechanism leads to the appearance of other sulfur atoms, and the tetragonal blocks

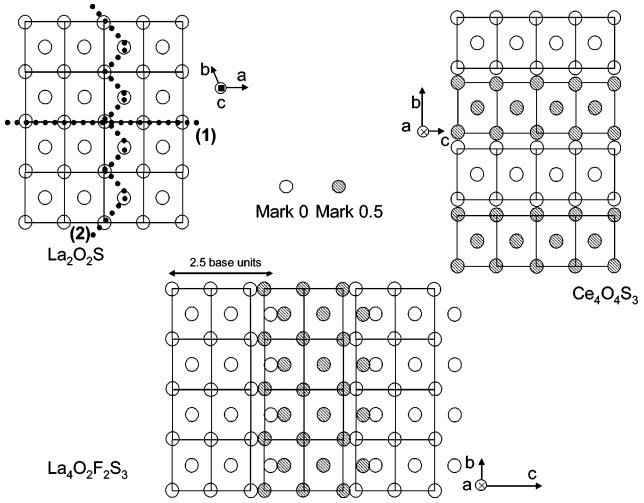

Figure 11. Representation of La2O2S, $Ce_4O_4S_3$ ($La_{4-x}Y_xO_2F_2S_3$), and $La_4O_2F_2S_3$ structures considering sulfur atoms and its tetragonal base unit. The shear directions are also represented by dot lines.

are separated by 0.9 Å. The structure of the $La_4O_2F_2S_3$ compound cannot be explained by a single shear plane. Indeed, the combination of two shearing planes $(100)_h$ and $(110)_h$ of the La_2O_2S hexagonal unit cell (dot line (**2**)) or $(011)_t$ and $(0\bar{1}1)_t$ of the previous tetragonal unit cell is necessary for describing the formation of $La_4O_2F_2S_3$ from La_2O_2S networks. The shear mechanism occurs every two and half tetragonal unit celld along the b_t axis with a $^1/_2$ a_t vector or a $^1/_2$ c_h vector translation. This geometrical operation generates other sulfur atoms, and the two blocks on either side of the shear planes penetrate each other.

The $Ce_4O_4S_3$ and $La_4O_2F_2S_3$ compositions are close, but the shearing mechanisms at the origin of the formation of these structures from Ln_2O_2S units are completely different (Figure 11). This is likely due to the occurrence of two cerium oxidation states (Ce^{4+}/Ce^{3+}) occupying various crystallographic sites in $Ce_4O_4S_3$. The trivalent cerium polyhedra are constituted by three oxygen atoms around 2.45 Å and five sulfur atoms at distances varying from 2.94 to 3.04 Å. The tetravalent cerium are more distorted and the four Ce(IV)−O bond lengths are shorter (2.17 Å < $d_{Ce(IV)-O}$ < 2.40 Å), whereas the dispersion of the four Ce(IV)−S bond distances is high (2.79Å < d(Ce(IV)−S) < 3.33 Å). Because of the large difference between Ce(III) and Ce(IV) coordination spheres, the shear mechanism operates preferentially around the larger Ce(III) site, breaking the less covalent bonds. In the $La_4O_2F_2S_3$ modulated structure, there is only one crystallographic site occupied by lanthanum cations, which have the same size as trivalent cerium. The shear operation then occurs not only along one peculiar plane as in $Ce_4O_4S_3$ but may act along two opposite planes in order to keep a large number of anions and a suitable geometry that will become modulated. An alternate sequence of two shear planes indeed appears around La atoms. This peculiar shear mechanism, as shown in Figure 11, could occur randomly along these two planes but the sequence is periodic and at the origin of the modulation of the structure. The alternance of the shear planes occurs regularly; after the so-called modulation point, this sequence is reversed and grows in opposite directions. The modulation point corresponds to the center of the smallest ribbon in the 3D supercell representation with layers of five sulfur atoms and $La_3(O,F)_3$ blocks (Figures 9 and 12).

To modify these structural features and attempt to obtain related commensurate structure, we have undertaken the substitution of La^{3+} by Y^{3+} ions where both these cations exhibit the same ionic size as trivalent and tetravalent cerium, respectively. The $La_3YO_2F_2S_3$ and $La_2Y_2O_2F_2S_3$ compounds adopt the same structural type as that of $Ce_4O_4S_3$ compound. Thus, in these commensurate networks, it is interesting to compare the interatomic distances. For the $La_3YO_2F_2S_3$ compound, the dispersion of bond distances is the highest. It is relevant to notice that the first site containing La^{3+} cations that are mainly affected by the shear mechanisms are highly distorted, with a largest La−S distance up to 3.15 Å and smaller La−O/F bond lengths at 2.33 Å. The second site containing Y^{3+} and La^{3+} cations also exhibits distortions with larger La(Y)−S = 3.03 Å and La(Y)−O/F = 2.46 Å bond distances. As far as the $La_2Y_2O_2F_2S_3$ compound is concerned, both the cationic sites become more regular, with La−S bond distances varying from 2.97 to 3.06 Å, La−O/F distances from 2.50 to 2.54 Å, Y−S bond lengths from 2.77 to 2.94 Å, and finallyY−O/F lenghts from 2.20 to 2.26 A. Such an evolution of the rare earth environment and especially the increase in the local distortion with La^{3+} content are in good agreement with the appearance of the modulation in the $La_4O_2F_2S_3$ compound and the description of various polyhedra observed in the related supercell.

Conclusions

A new class of compounds, the rare earth oxyfluorosulfides $La_{4-x}Y_xO_2F_2S_3$ (x = 0, 1, 2) has been prepared by a solid-state route and exhibits outstanding structural features. The crystal structures of different compositions have been determined on the basis on electronic diffraction and X-ray powder diffraction patterns. $La_4O_2F_2S_3$ has an incommensurate modulated structure with a modulation vector q^* = 0.2607 c*, whereas the $La_3YO_2F_2S_3$ and $La_2Y_2O_2F_2S_3$ compounds exhibit the same structural features as the orthorhombic unit cell (space group *Pbam*) of the $Ce_4O_4S_3$ composition close to that of the previous one. The description of the modulated structure of $La_4O_2F_2S_3$ in the 4D space reveals the occurrence of various polyhedra with two main environments similar to those observed in $Ce_4O_4S_3$. The La−X(O/F,S) bond length dispersion has been followed along the modulation. To better visualize the La polyhedra sequence and the intergrowth of shells and ribbons, we have obtained a 3D approximation of $La_4O_2F_2S_3$ by considering a supercell with 43 atoms in various crystallographic sites. There are two La polyhedra along the sequence where the dispersion of the La−X (X = O/F,S) bond length is the smallest, corresponding to the most regular environments (2.33 Å ≤ $d_{La-O/F}$ (4) ≤ 2.43 Å, 3.07 Å ≤ d_{La-S} (5) ≤ 3.30 Å. Around these two polyhedra, the modulation can grow, leading to a various number of O/F and S atoms surrounding lanthanum and various bond distances. Finally, two main La environments can be distinguished along this sequence, with 4 O/F atoms and 5 S atoms for the larger sites and 4 O atoms and 4 S atoms for the smaller sites. One should note that this latter site is not strongly affected by the modulation,

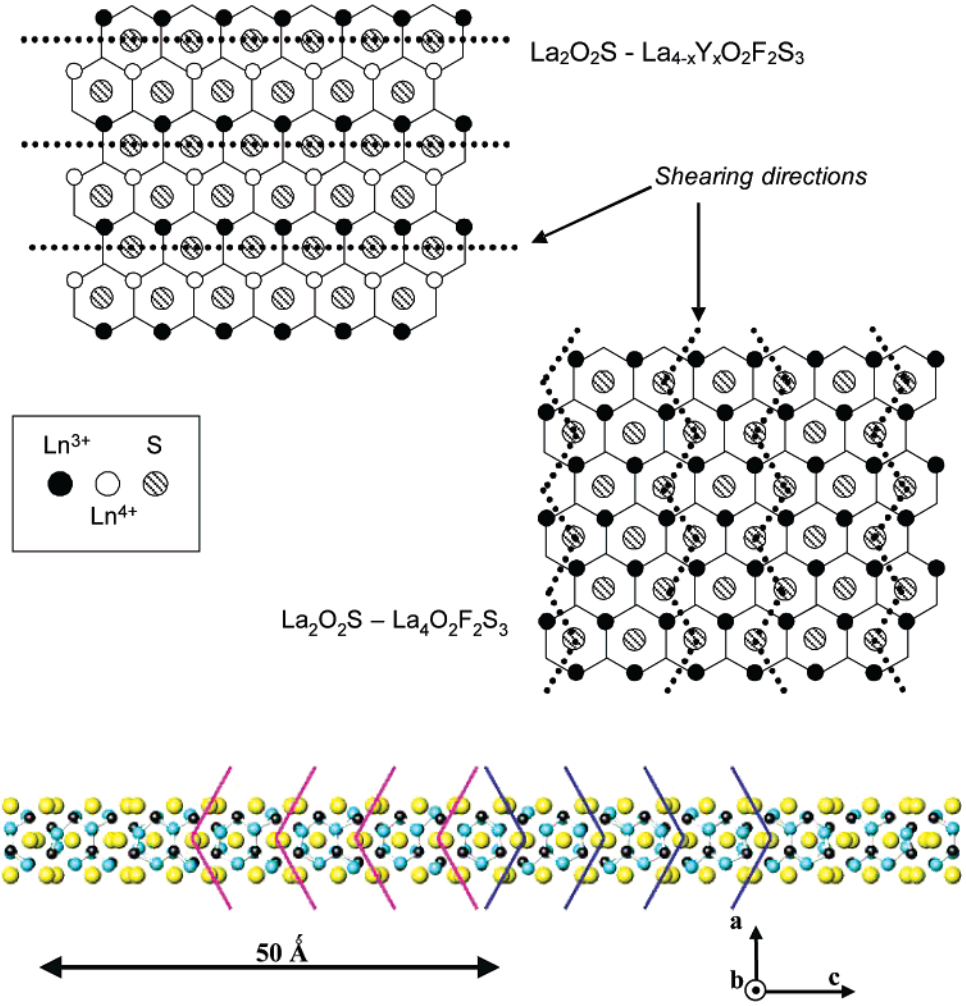

Figure 12. Representation of shear planes in the La_2O_2S type structure leading to the formation of commensurate structure and $La_4O_2F_2S_3$ incommensurate modulated structure. The shear planes are also represented along the supercell of the $La_4O_2F_2S_3$ compound.

the variation of La−X (X = O/F, S) bond lengths being sufficiently small along the modulation. On the other hand, the largest sites with 5 sulfur atoms exhibit high variation of La−X bond lengths along the modulation, namely, a reduction of La−O/F bond lengths followed by an increase in La−S bonding and vice versa. The $La_{4-x}Y_xO_2F_2S_3$ structures can be described as the intergrowth of $[La_n(O/F)_n]$ and S_m finite ribbons. The size of the ribbons, depending on the number of atoms, varies in the commensurate and the incommensurate modulated structure. The relationships between these structures and the La_2O_2S network have been explained by shearing mechanisms, as has the origin of the $La_4O_2F_2S_3$ structure modulation. This outstanding variation of the structure is indeed due to the large ionic size of the rare earth ions, i.e., the environments of lanthanum atoms that can locally be affected by the shear planes. There is actually a competition between the formation and the orientation of these shear planes, leading to the increase in the number of sulfur atoms in the vicinity of the rare earth ion, and the strong constraints create a modulation of La−S and La−O/F bond distances. The introduction of Y^{3+} cations substituting for larger La^{3+} ions and creating more covalent bonds limits the development of the shear planes in various directions, and commensurate structures can be stabilized. The modulation can indeed be annihilated by introducing small rare earth ions such as Y^{3+} cations as a substitute for larger La^{3+} ions. This leads to the creation of a single shear mechanism around La^{3+}, whereas the smaller rare earth sites preferentially occupied by Y^{3+} are not directly affected by this operation. This is the first time that a displacive and occupation modulation of a 3D structure due to the occurrence of large rare earth ion and mixed anion (F, O, S) have been explained considering shear mechanisms and constraints around the rare earth atom. Finally, these unusual structural features should give interesting electronic and optical properties.

Acknowledgment. This work has been supported by Rhodia Chimie (Centre de Recherche d'Aubervilliers-France).

CM0510817